remote sensing

MDPI

Article

An Erosion-Based Approach Using Multi-Source Remote Sensing Imagery for Grassland Restoration Patterns in a Plateau Mountainous Region, SW China

Guokun Chen [1,2], Yiwen Wang [1,*], Qingke Wen [3], Lijun Zuo [3] and Jingjing Zhao [1]

[1] Faculty of Land Resource Engineering, Kunming University of Science and Technology, Kunming 650093, China; chengk@radi.ac.cn (G.C.)
[2] Key Laboratory of Plateau Remote Sensing, Yunnan Provincial Department of Education, Kunming 650093, China
[3] Aerospace Information Research Institute, Chinese Academy of Sciences, Beijing 100101, China
* Correspondence: yven@stu.kust.edu.cn

Abstract: Satellite remote sensing of grassland ecosystem restoration requires considering both the above-ground biomass and soil information, and the latter is even more crucial due to the value and restoration difficulty of soil productivity. In this study, we proposed an approach to support the restoration pattern for mountainous grasslands at regional scale. The approach integrates different aspects and key processes, including degradation status, restoration potential and recovery capability, compared to a reference state. Specifically, we illustrated the method with the case of grasslands in southwestern China from a conservation perspective. Soil erosion conditions, net primary productivity and regrowth rate of grasslands were selected as indicators to reveal restoration possibilities. The results showed that the method proposed for remote sensing identification of grassland distribution has an overall accuracy of 88.21% at the regional scale. 59.54% of grasslands in Zhaotong are being eroded with an unsustainable erosion rate greater than the tolerant soil loss, and the average annual soil erosion rate is 952.17 t/(km^2·a). Meanwhile, there is obvious spatial heterogeneity in soil erosion factors, vegetation restoration potential and regrowth rate, and the dry–hot valley of Jinsha River in the southwest is much more sensitive to climate change and vulnerable than other regions. The grassland vegetation cover revealed a fluctuating trend and protection of grassland vegetation on soil from erosion has an obvious lag, restoration efforts should be focused on the months before the arrival of the rainy season. In light of various grassland types, the overlay zoning results suggest various restoration patterns of natural repair and manual intervention should be employed for different grasslands. Urgent action is needed to face the challenge and process of grassland degradation and restore its sustainability with shared understanding by taking the stakeholders, collaborations and mutual relationships among different roles into account (e.g., scientist, government and herdsman).

Keywords: CSLE model; grassland erosion; random forest; remote sensing identification; restoration mode; restoration potential

Citation: Chen, G.; Wang, Y.; Wen, Q.; Zuo, L.; Zhao, J. An Erosion-Based Approach Using Multi-Source Remote Sensing Imagery for Grassland Restoration Patterns in a Plateau Mountainous Region, SW China. *Remote Sens.* **2023**, *15*, 2047. https://doi.org/10.3390/rs15082047

Academic Editors: Ernesto López-Baeza, Francisco García-Sánchez, Ana Perez Hoyos and Carlos Doménech

Received: 27 February 2023
Revised: 28 March 2023
Accepted: 10 April 2023
Published: 12 April 2023

1. Introduction

Grasslands support a large fraction of terrestrial biodiversity and take up about 40% of the Earth's land area [1,2], and play essential roles in conserving soil and water, ensuring food security and creating a strong ecological barrier [3–5]. However, due to agriculture, urbanization, invasive species, climate change and human activities, about 49% of the grasslands worldwide have been degraded to varying degrees [6–8], posing a major threat to the ecosystem functions and services maintaining, which further hinders the achievement of goals such as the United Nations Decade on Ecosystem Restoration and the Sustainable Development Goals (SDGs) [3]. In southern China, grasslands are mostly distributed in the mountainous or hilly regions such as Yunnan, Guizhou and Sichuan. They are

large in area, evergreen during all seasons, high in grass yield and have both production and ecological functions. Despite the importance of the grassland ecosystem and the environmental implications of its degradation, the status quo is not taken seriously [9]. Subjected to hydrothermal and topographic conditions, the restoration efforts in southern China are insufficient, and the development of the grassland-related industry is slow [10]. To some extent, the restoration of grassland in southern China is a major breakthrough in the construction of sustainable grassland husbandry, given the challenging conditions of continuous degradation and desertification of the northern grasslands.

So far, the causes, consequences and processes of grassland restoration have been widely studied from different perspectives with various indicators [11]. However, vast grasslands continue to degrade, and the restoration effect has no uniform law. The effect of a single restoration measure for grassland ecosystems is limited, and the effect of the same restoration measure varies greatly under different circumstances, which makes it difficult to choose and learn from practical application. The major reasons behind it can be summarized as follows [3,7,12,13]: Firstly, the complex broken plateau mountainous terrain, the cloudy and rainy weather and data availability bring difficulties to the identification of detailed grassland distribution at the regional scale. Besides, remote sensing assessment of grassland degradation has been hampered by differences in definitions, classifications, inconsistencies in the drivers of different types of degradation across and within regions, as well as limited linkages between satellites and those unobserved variables [3]. Meanwhile, grasslands have inconsistent interests from different perspectives and roles. Different stakeholders need different functions and services from grasslands, carbon sequestration, biodiversity, products and the raw materials produced, but it is impossible to get all of them from one place [14]. Besides, there is a lack of shared understanding on grassland policies and regulations for long-term sustainability among different roles. Lastly, mountainous areas are more sensitive to climate change and human activities, which has accelerated this degradation to a greater extent than any other areas [14,15].

Therefore, it is necessary to propose an approach to achieve regional or large-scale grassland restoration goals [9,16], and the approach should consider regional ecological environmental characteristics (such as vegetation dynamics, precipitation, topography and soil condition), the causes of grassland degradation, the influence of climate change and human activities on grassland, the recovery mechanisms and capabilities of different ecosystem types, and finally formulate targeted ecological restoration modes for different types of grasslands [9,17]. Specifically, for the plateau mountainous areas, several aspects should be highlighted, to clarify the spatial distribution of grasslands at the regional scale with high resolution, to evaluate driving factors and the degree of grassland degradation, and to describe the grassland restoration potential and space and speed quantitatively. Only in this way can we optimize the community structure accurately, and improve the functions, biodiversity and stability of the grassland ecosystems.

Regional-scale grassland monitoring is the premise and basis for the scientific utilization of grasslands and implementation of ecological restoration. As grasslands in plateau mountainous areas are generally fragmented, it is difficult to identify them only through field surveys or medium–low resolution optical remote sensing imagery [18]. In addition, existing grassland distribution data are mainly retrieved from national or global land cover datasets, and the accuracy cannot meet the needs of targeted research [19,20]. Thus, constructing an integrated remote sensing method to accurately identify the distribution of fragmented grasslands is of great importance. Related studies confirmed that the accuracy of remote sensing classification largely depends on sample selection and the input features [21–23]. The spatial uniformed sample selection is well representative, which can cause positive impacts on classification results [24,25]. Meanwhile, using time series features as input features can effectively solve the problem of the 'same spectrum but different objects' [26–28], and adding terrain features of the grassland distribution is also crucial to improve the classification accuracy [29].

For grassland degradation itself, any definition of it is essentially a grassland sustainability issue [3]. Vegetation is closely related to soil. Vegetation degradation will lead to soil degradation and environmental degradation. Soil degradation and harsh environments will further aggravate vegetation degradation, showing a vicious cycle. Therefore, a good soil ecosystem is the fundamental guarantee for the sustainability of mountain vegetation. At present, soil erosion is the most important land degradation problem in mountainous areas of southern China [30]. Many scholars have used empirical models, such as USLE [31], RUSLE [32] and CSLE [33], to monitor soil erosion in different regions and spatial ranges. Nevertheless, there are still some shortcomings, since most models are developed based on a large number of plots or slope observation data. When applied at the regional scale or larger scales, the establishment conditions of model, the characteristics of the applicable objects and the requirements for input variables or parameters should be simplified accordingly, and the reliability of the results is often questioned [34,35]. Restricted by the heterogeneity and interaction of erosion factors, the data access and quality in plateau and mountainous areas have become the bottleneck of quantification of erosion at large scales [36,37]. Lastly, most soil erosion assessments focus on cultivated land using multi-year average erosion modulus as a quantitative index, and the analysis of soil loss across seasons is insufficient. To some extent, a fine quantification of grassland erosion can not only reflect the degradation degree, trend and limiting factors of the grassland, but also the basis for timely, appropriate and moderate ecological restoration in the future.

Grassland restoration should also answer the questions of whether ecological restoration is natural restoration or manual intervention, when, where and to what extent of the efforts should be made. When faced with a degraded ecosystem, the first consideration is to determine its ability to revert to a certain targeted condition, that is, to evaluate the magnitude of the restoration potential [38,39]. For studies of vegetation's restoration potential (RP), the restoration target is usually defined according to the principle of 'habitat similarity', and the RP is often determined by measuring the 'gap' between the degraded community and the reference community [40,41]. These methods are simple and feasible, but fail to fully consider the impact of micro-topographic changes on habitat conditions, and are impracticable at the regional scale [42]. With the quick development of satellite and remote sensing technology, high-resolution remote sensing images are capable of quantifying vegetation cover, biomass, productivity and other surface characteristics [13,43]. As climate change and human activities are two major factors leading to changes in terrestrial ecosystems [44,45] and the net primary productivity (NPP), which is the total organic matter amount accumulated by plants through photosynthetic conversion, can accurately reflect these two factors [46]. Until now, there have been several methods to estimate NPP, such as the normalized difference vegetation index (NDVI), the enhanced vegetation index (EVI), the soil-adjusted vegetation index (SAVI) and the fraction of photosynthetically active radiation (FPAR) and leaf area index (LAI), among which NDVI may be the most effective one to reflect the restoration potential [3,47–50]. As for the recovery speed of grasslands, it is usually represented by the regrowth rate and determined by the hydrothermal conditions of the region.

Yunnan province harbors most of the biodiversity in China due to diverse climatic conditions and various ecosystems. Nevertheless, with the interference of socio-economic activities, the grassy hills and slope patches have been demonstrated with degrading features, such as a low grass layer, sparse vegetation and low grass yield [51], which is quite representative for mountainous grasslands in Southern China. The aim of this study is to propose a grassland restoration approach based on the restoration goal, realization speed, space and limiting factors of grassland degradation. Specifically, we aimed to monitor and identify grasslands, quantify grassland erosion, evaluate the restoration potential and regrowth rate and further clarify the grassland restoration pattern quantitatively with the aid of field investigation and multi-source remote sensing imageries.

2. Materials and Methods

2.1. Study Area and Data Sources

Yunnan province has the largest proportion of natural grasslands in southwest China, with an area of 134,630 km^2, accounting for about 37.84% of the southwest grassland area [52]. The Zhaotong municipality in Yunnan has a relatively dense distribution of grassland, and was selected as the study area (Figure 1). Zhaotong lies between 102°52′–105°19′E and 26°55′–28°36′N, on the right bank of the lower reaches of the Jinsha River (main stream of the Yangtze River) and in the foothills of the Wumeng Mountains, with a total land area of 23,000 km^2. Located in the transition zone from the Sichuan Plain Basin to the uplifted Yunnan–Guizhou Plateau, the altitude is high in the south and low in the north, and high mountains and deep valleys characterize the region. The climate varies greatly at different altitudes, and the spatial and temporal distribution of rainfall is extremely uneven, mainly concentrated in the rainy season from May to October. The range of average annual temperature is 11–21 °C and the range of average annual precipitation is 660–1230 mm [53]. Soil erosion in this region is extremely serious, mostly in the form of rainstorm and strong surface runoff. Typical vegetation includes subtropical coniferous forests, broad-leaved forests, shrubs and grasslands. The major soil groups (FAO/UNESCO classifications) in the study area are Acrisols, Cambisols, Luvisols and Alisols. However, the current grassland husbandry scale in the region is poor, with beef and sheep meat accounting for only 7.34% of total meat products in the city, which has not yet fully utilized its vast grassland resources [54].

The critical data used for regional scale grassland identification in Zhaotong are listed as follows: (1) the multi-source remote sensing data of Landsat–8/OLI (30 m), Sentinel–2 A/B (10 m), and Sentinel–1 (10 m) used to construct complete time series datasets, GF–1 (10 m) data obtained from the China Earth Observation Shared Data Platform; (2) ALOS DEM with a spatial resolution of 12.5 m, obtained to acquire topographic input features; (3) six non-homogenous remote sensing data [55–60] on grassland information used in the sample selection, detailed information is shown in Table 1; (4) 117 investigated grassland parcels were used for accuracy verification collected from the national survey (Figure 1), and 112 non-grassland verification samples were determined by the interpretation of Google Earth images on the GEE platform.

Table 1. Detailed information of the six non-homogenous land use products.

Name	Resolution	Mapping Accuracy
1:100,000 land use data	30 m	85%
GlobeLand30 data	30 m	83.50%
CGLOPS–1 data	100 m	80%
GLC_FCS30 data	30 m	82.50%
FROMLC data	10 m	72.76%
China 1:1,000,000 vegetation map	30 m	64.8%

Data used to evaluate the vegetation RP consists of two parts: (1) NPP datasets (2000–2020) from Global LAnd Surface Satellite (GLASS) products; (2) precipitation and temperature data for the period 2000–2020 used to calculate the potential net primary productivity (PNPP) (Table 2). Data used to evaluate soil erosion includes: (1) 109 primary sample units (PSUs, Figure 1) in Zhaotong in the Fourth National Soil Erosion Survey conducted by the Ministry of Water Resources of China (MWRC). PSUs were determined using a stratified unequal probability surface sampling method. Each PSU is a small watershed for field investigation and data collection on soil-erosion–related index information, and the data collected concerning soil erosion affecting factors share uniform standards and specifications, and were well-examined in every step of the survey. Based on PSUs with grassland parcels, information such as FVC every 15 days, rotations, terraces and grassland type, were also investigated on site. For different elevation zones and grassland types, we generated FVC dynamic curves across the year, which are employed to fulfill the absence of image data caused by cloudy and rainy weather, as well as the complex terrain

conditions in our study area; (2) Thematic data for calculating regional soil erosion factors (Table 2). All these data were preprocessed and resampled to a 10 m spatial resolution for further analysis.

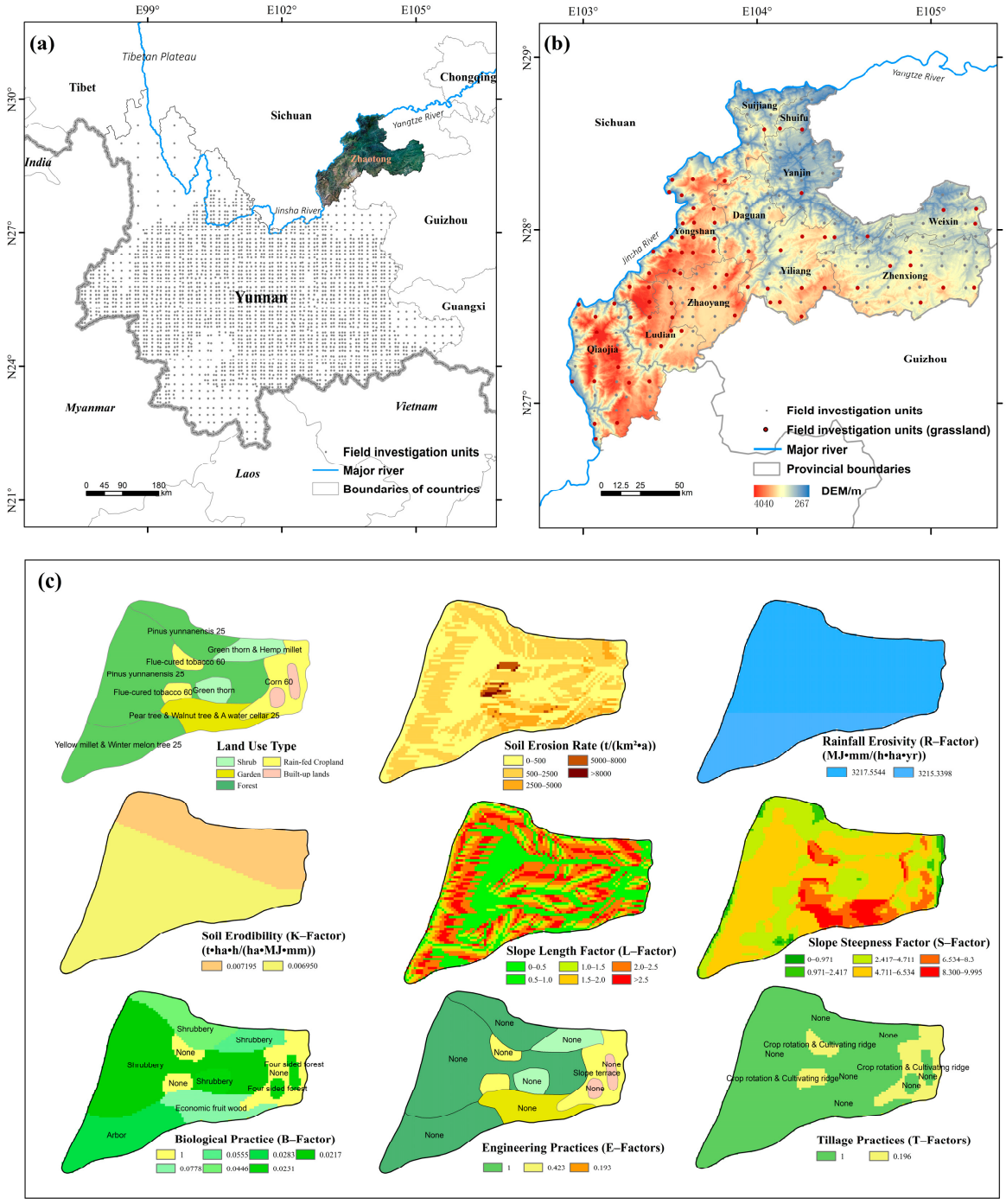

Figure 1. (**a**) Primary sample units (PSUs) allocated in Yunnan with different sampling densities; (**b**) Map of the Zhaotong municipality, showing location, altitude variation and the major river in the region; (**c**) Example of PSUs (PSU No.5332220126).

Table 2. List of the major multi-source data in this study.

Name	Source	Resolution
NPP dataset (2000–2020)	GLASS products, University of Maryland (http://www.glass.umd.edu, accessed on 1 September 2022)	500 m
World Clim	https://www.worldclim.org/data/monthlywth.html, (accessed on 4 December 2022)	1000 m
Monthly temperature data	National Earth System Science Data Center	1000 m
Daily erosive rainfall events across three decades (1990–2020)	National Meteorological Data Sharing Center	Resampled to 10 m
Soil erodibility	Beijing Normal University	Resampled to 10 m
ALOS DEM data	https://search.asf.alaska.edu, (accessed on 28 February 2022)	12.5 m
Vegetation coverage	Sentinel images	10 m
Detailed soil conservation measures in PSUs	The Fourth National Soil Erosion Survey in China	10 m

2.2. Grassland Distribution Identification Based on the Random Forest Algorithm

The experimental design of grassland remote sensing identification in the study area is shown in Figure 2, which is mainly composed of three steps [61]: (1) sample selection optimization; (2) determination of input features and optimization; (3) image classification and accuracy verification.

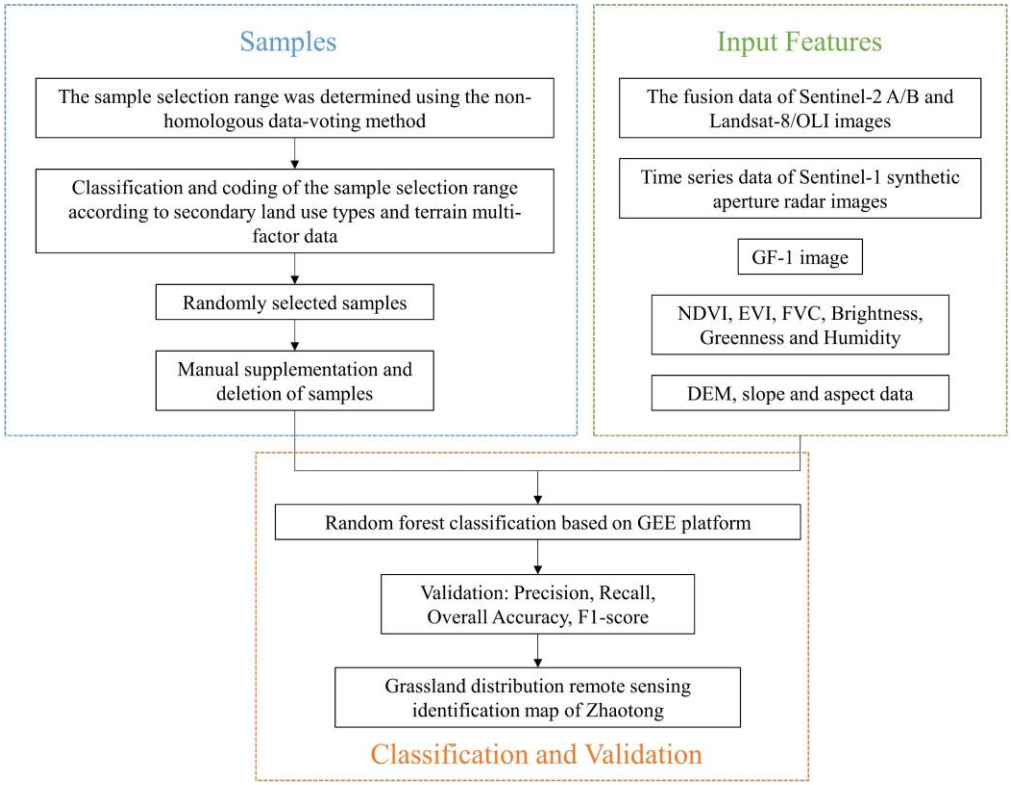

Figure 2. Experimental design of grassland remote sensing identification at a regional scale.

Since the number, distribution and representativeness of training samples have a significant impact on the accuracy of image classification and recognition results [62], a non-homogenous data-voting approach was employed to select the training samples instead of retrieving from a single-source dataset. We also referred to the GlobeLand30 classification system and existing land-use types in the region, and divided them into six categories. Consecutive pure pixels with the same land use type in six non-homogeneous land-use products were used to determine the sample selection range, which was divided

and coded according to an overall consideration elevation, slope and slope direction of land-use types. Grids of 30 × 30 m were further used to traverse the coded selection range, and those with different coding types were set as the final sample selection. Considering the randomness, sample points are further created for each type by controlling the allowable distance between samples. Finally, we supplemented the selection for regions lacking samples by using Google Earth images, an NDVI time series curve, as well as a vegetation map of China. The final samples obtained for farmland, forests, grasslands, water bodies, built-up areas and bare land were 1162, 627, 500, 65, 134 and 39, respectively.

It is challenging to acquire complete time series data for grasslands in mountain regions of southwest China because of the cloudy and rainy weather. The multispectral time series dataset fused with Landsat–8/OLI and Sentinel–2 A/B data is used as input features. The median data of the corresponding months of the year before and after 2020 were used as a supplement to improve the coverage. To solve the problem of the incomplete regional coverage, the multispectral and radar time series data of Sentinel–1 were added as input features. In addition, considering the fact that the distribution of grasslands had typical topographic features, the topographic factors were also used as input features, which is conducive to reducing the grassland omission problem.

Random Forest (RF) is a non-parametric machine-learning algorithm, which consists of multiple CARTs, which can effectively run a large number of datasets and process thousands of input variables [63]. In this study, a total of 2527 sample points and 67 input characteristic bands were involved. Because of the large volume of samples and input features, we conducted the RF classification process on the high-performance cloud computing platform GEE. In this study, the hyper parameters used to train the random forest model in the process of grassland classification and recognition include *numberOfTrees*, *variablesPerSplit*, *minLeafPopulation*, *bagFraction*, *maxNodes* and *seeds*. The *numberOfTrees* start number was set to 10, the termination number was set to 200, and the loop iteration was performed with 10 as the step size. When *numberOfTrees* equals to 150, the classification accuracy reaches the maximum, so the optimal value of the decision tree was set to 150. Characteristic variables, such as spectrum, vegetation index, texture, vegetation coverage and terrain (elevation, slope and aspect), were constructed and sorted. Finally, bands of Blue, Green, Red, NIR and SWIR, NDVI, EVI, FVC, Brightness, Greenness and Humidity were used as the major input feature variables for the final classification. Four accuracy metrics of Precision, Recall, Overall Accuracy (OA) and F1 score were calculated based on the validation data (117 grassland and 112 non–grassland validation samples). The closer the value of the above four indicators is to 1, the better the grassland recognition is, and the specific formulas are as follows:

$$\text{Precision} = \frac{\text{T1}}{\text{F1} + \text{T1}}, \tag{1}$$

$$\text{Recall} = \frac{\text{T1}}{\text{F2} + \text{T1}}, \tag{2}$$

$$\text{Overall Accuracy} = \frac{\text{T1} + \text{T2}}{\text{F2} + \text{T1} + \text{F1} + \text{T2}}, \tag{3}$$

$$\text{F1 score} = \left(1 + \beta^2\right) \frac{\text{Precision} \times \text{Recall}}{\text{Precision} + \text{Recall}}, \beta = 1, \tag{4}$$

where T1 refers to the numbers that are correctly extracted as positive examples, F1 is the numbers that are not correctly extracted as negative examples, F2 is the numbers that are not correctly extracted as positive examples, and T2 is the numbers that are correctly extracted as negative examples.

2.3. CSLE Model

On the basis of USLE, Liu et al. [33] proposed the Chinese soil loss equation (CSLE) model based on numerous measured plot data in China. The model described a mathematical relationship between soil erosion rates and the erosion factors, and can be modified based on regional conditions, and has been widely used and verified for the last two decades [64]. The greatest advantage of CSLE is that the actual mountainous condition and complex soil and water conservation measure systems in China are considered in detail, with the C factor and P factor in USLE being modified into three factors of B factor, E factor and T factors. It is also the methodological basis of the Fourth National Soil Erosion Survey in China and the official model of the Ministry of Water Resources of China. The CSLE formula is defined as follows:

$$A = R \times K \times L \times S \times B \times E \times T, \quad (5)$$

where A is the average annual soil loss, $t/(hm^2 \cdot a)$; R is the average annual rainfall erosivity ($MJ \cdot mm/(hm^2 \cdot h \cdot a)$), K is the soil erodibility, ($t \cdot hm^2 \cdot h/(hm^2 \cdot MJ \cdot mm)$), L and S are the slope length and slope steepness factors, respectively, dimensionless, B, E, T are soil conservation measures of biological, engineering and tillage, respectively, dimensionless.

The calculation methods of R, K, L and S factors are detailed in the related literature [65–67]. L was calculated using the slope length index proposed by Liu et al. [68]; S was calculated based on 12.5 m DEM data with slopes below 10° using the formula of McCool et al. [69], and above 10° according to Liu et al. [70], a verified study on steep slopes from 9° to 55°. E and T were assigned by widely collected local experiments and combining them with field investigation.

Specially, the impact of vegetation on conserving soil has been well recognized. To account for vegetation, the B factor has been used in the CSLE to monitor erosion. Similar to the C factor in USLE, B values are weighted average soil erosion ratios (SLR_i), each of which represents the ratio of soil erosion under current conditions to the soil loss under unit plot conditions during the same period [64,67]. SLR_i changes as vegetation cover changes during the process of plant growth. The B value then represents the average of the SLR_i values, each weighted by the rainfall erosivity portion. B was firstly obtained by using a combination of sentinel data, meteorological satellite data and ground survey to obtain the vegetation cover of the grassland in Zhaotong for the 12 months throughout the year, and then calculate the soil loss ratio SLR_i for each month, to acquire the annual average B values. For grassland, B is calculated as follows:

$$B = \sum_{i=1}^{12} SLR_i \times WR_i, \quad (6)$$

$$SLR_i = \frac{1}{1.25 + 0.78845 \times 1.05968^{100 \times FVC}}, \quad (7)$$

where SLR_i is the proportion of soil loss of the grassland during month i, dimensionless, the value range is 0–1; WR_i is the proportion of rainfall erosivity in the month i to the whole year, and the value range is 0–1; fractional vegetation coverage (FVC) is the vegetation cover calculated based on the NDVI, and the value range is 0–1.

2.4. Grassland Regrowth Capacity and Net Primary Productivity

According to previous onsite investigations in the National Grassland Survey, the grassland in Zhaotong can be divided into four vertical zones based on altitude and hydrothermal conditions, which are thermal grassland (−800 m), with a regrowth rate of 30%; warm grassland (800–2100 m), with a regrowth rate of 20%; temperate rangeland (2100–3800 m), with a regrowth rate of 15%; and alpine rangeland (3800–4300 m), with a regrowth rate of 5%.

Characterized by spanning large spatial areas with multiple resolutions, RS monitoring of NPP has been applied and is still an effective way to indicate grassland conditions [3].

The grassland RP, which reflects the space of ecological restoration, is defined as the gap between the actual net primary productivity (ANPP) and PNPP, and the formulas are listed as follows:

$$PNPP_m = \max_{2000 \le i \le 2020} \{PNPP_i\}, \quad (8)$$

$$RP = PNPP_m - \frac{1}{21} \sum_{i=2000}^{2020} ANPP_i \quad (9)$$

In this study, the ANPP was derived from the Global LAnd Surface Satellite (GLASS) products, while the PNPP was estimated using the Thornthwaite memorial (TM) model, which incorporates a revised variant of the Thornthwaite potential evapotranspiration model into the Miami model, and its effectiveness has been confirmed in previous studies [71,72]. Concretely, based on the relationship between evapotranspiration and carbon sequestration, the TM model estimates that the PNPP has better performance than the Miami model [73]. PNPP is calculated by the following equations:

$$PNPP = 3000[1 - e^{-0.0009695(v-20)}], \quad (10)$$

$$v = \frac{1.05r}{\sqrt{1 + \left(1 + \frac{1.05r}{L}\right)^2}}, \quad (11)$$

$$L = 3000 + 25t + 0.05t^3, \quad (12)$$

where PNPP refers to the potential net primary productivity (g C/m^2), v is the actual mean evapotranspiration (mm), L refers to the mean evapotranspiration (mm), t is the mean temperature (°C) and r refers to the total precipitation (mm) annually.

2.5. Overlay Analysis for Grassland Restoration Zoning

The regrowth rate represents the rate of grassland recovery, while soil erosion is the limiting factor in the recovery process. Based on this, spatial overlay analysis for layers of the restoration potential, regrowth rate and soil erosion rate in the grassland area were conducted. Table 3 displays the zoning criteria based on the literature. Among them, the soil erosion rate of 500 t/(km^2·a) represents the tolerant soil loss, which is the maximum soil loss tolerance in southwestern China to maintain long-term soil fertility and basic stability of land productivity [74]. When the soil erosion rate exceeds the threshold value, the soil productivity is unsustainable. The annual average value of the restoration potential for decades in this region is also used as the threshold [75]. The regeneration rate of 20% is based on the research of husbandry, and the threshold is determined according to the local grazing intensity, population density, hydrothermal conditions and other policy factors [75]. Here, we integrate these three as a common standard to divide the grassland restoration zones in Zhaotong.

Table 3. Grassland regionalization criteria for ecological restoration.

Average Soil Erosion Rates t/(km^2·a)	Restoration Potential (g C/m^2)	Regrowth Rate (%)	
		≥20	<20
≤ 500 (Tolerate)	≥1350	A	B
	<1350	C	D
> 500 (Unsustainable)	≥1350	E	F
	<1350	G	H

3. Results

3.1. Grassland Distribution Identification at the Regional Scale in Zhaotong

The Remote Sensing identification results of the grassland in Zhaotong is revealed in Figure 3. With an overall accuracy of 88.21% and a spatial resolution of 10 m at the regional scale, the proposed approach is reliable for mountainous regions with fragmented grassland patches and complex terrain conditions compared to five other typical land-use products. Results show that grassland covers an area of 5132 km^2 and occupies about 23% of the total land area in Zhaotong. Affected by topography and hydrothermal conditions, the distribution area of grassland showed a significant decreasing trend from southwest to northeast, and a trend of first increasing and then decreasing as altitude and slope increase, with high values concentrated in the range of 1000–2000 m and a slope gradient of around 20°.

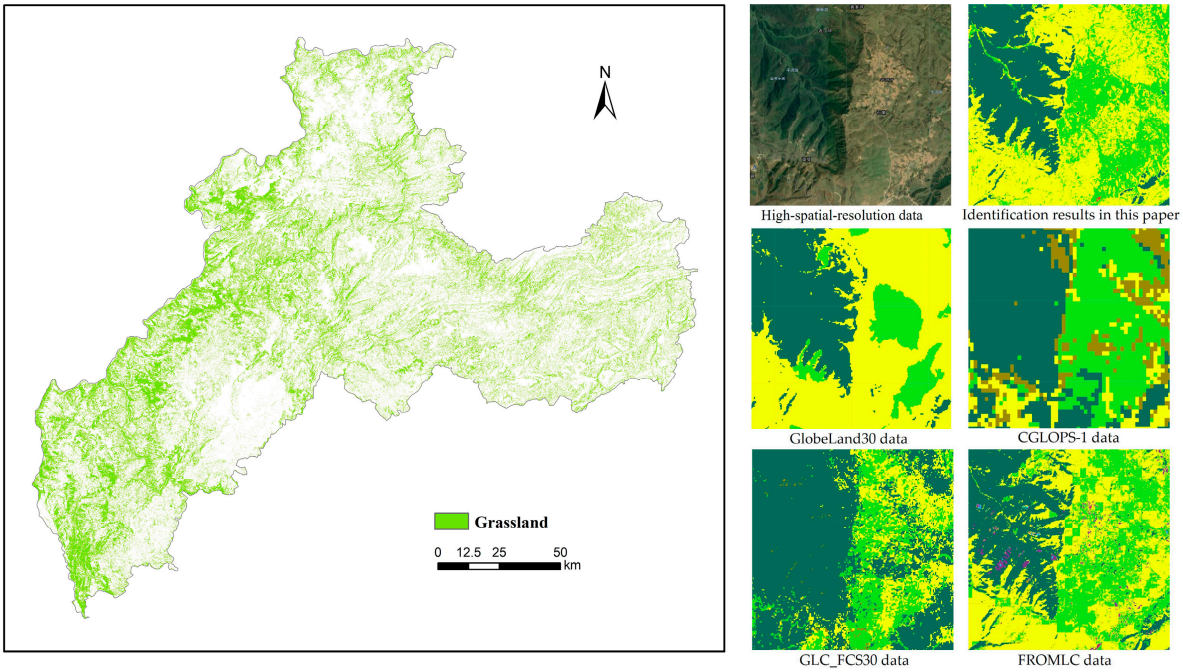

Figure 3. Remote Sensing identification map (10 m) of grassland distribution in Zhaotong in 2020.

Due to the strong altitudinal slopes in mountainous regions, meteorological, hydrological and ecological conditions (especially vegetation and soils) are more sensitive than others over relatively short distances. Alongside that, vegetation coverage information extracted from medium–low resolution images will cause different degrees of overestimation, and does not conform to the input requirement of many empirical models, such as USLE, RUSLE and CSLE. Considering that the critical role of vegetation cover in preventing soil erosion has been well recognized, we retrieved a monthly time series grassland FVC, with a resolution of 10 m across the year for the first time in this region, to reflect the vegetation characteristics of the grassland area more objectively. As can be seen in Figure 4, it is clear that the whole study area experiences higher FVC values during the warm seasons, especially from July to October. High FVC values are mainly found in the north and east, while low FVC values are mainly distributed in the west, especially in the dry–hot valley area of the Jinsha River. Compared to other regions, the western area also exhibits huge seasonal variation in the FVC, which is mainly because of the relative abundant precipitation in regions except the west. Obviously, the distribution area of the grassland is extremely uneven in both time and space.

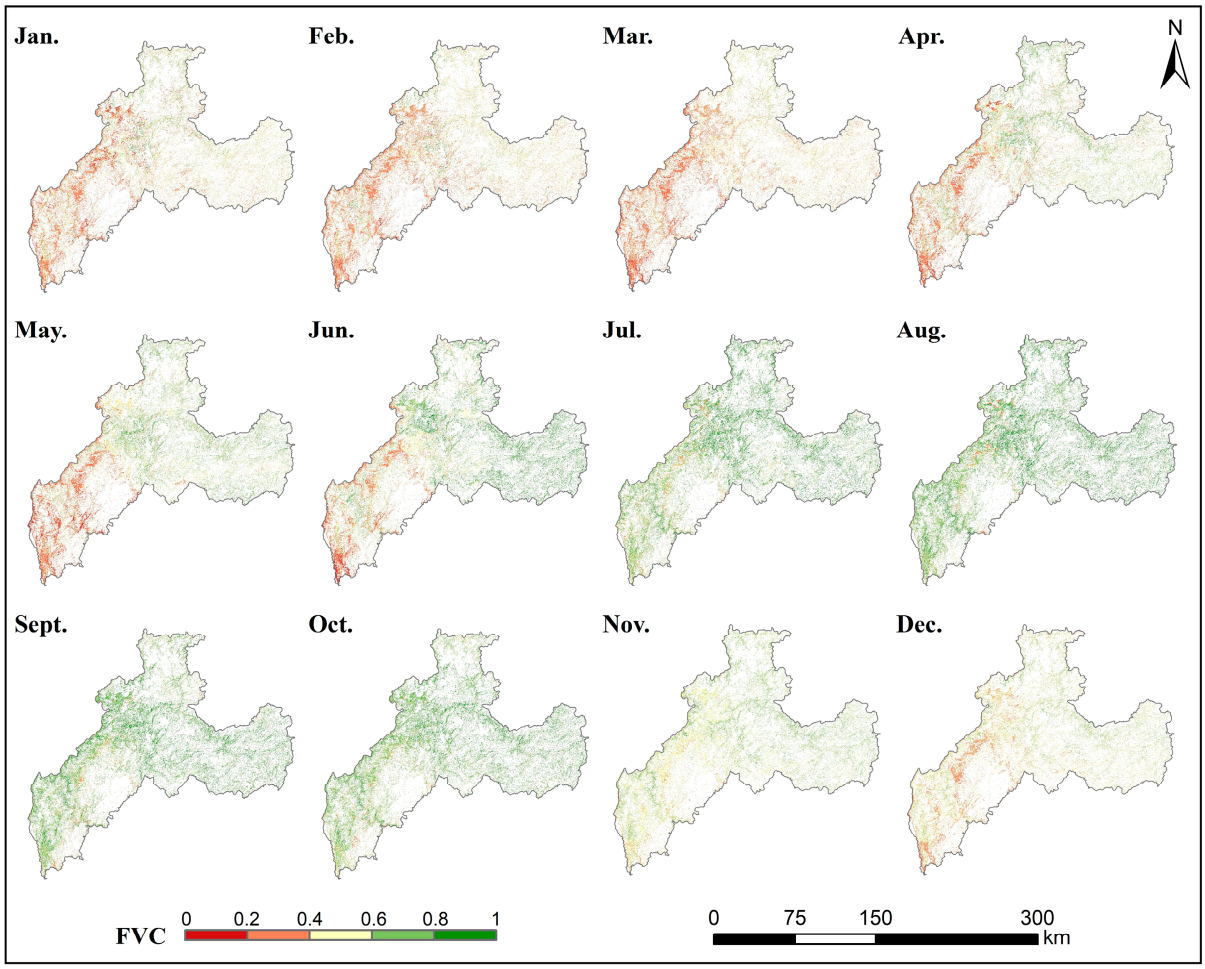

Figure 4. Monthly fractional vegetation coverage (10 m) of grassland in Zhaotong in 2020.

3.2. Spatial–Temporal Quantification of Grassland Erosion Using the CSLE Model

3.2.1. Distribution Characteristics of Soil Erosion Factors of CSLE

Among the factors affecting grassland erosion, the R factor (Figure 5a) generally showed a decreasing pattern from north to south, with a value range of 2749.30–4258.40 MJ·mm/(hm^2·h·a) and an average of 3124.25 MJ·mm/(hm^2·h·a). The K values (Figure 5b) in Zhaotong vary from 0 to 0.0099 t·hm^2·h/(hm^2·MJ·mm), with a mean value of 0.006 t·hm^2·h/(hm^2·MJ·mm), and the highest values were mostly found in Cambisols and Luvisols areas in the east. The L and S factors in Figure 5c vary from 0 to 45, with a mean value of 10.28. Higher LS values characterized the whole study area except for the Zhaoyang district in the south with relatively gentle slopes and less grassland distribution. The annual average value of the B factor in grassland areas (Figure 5d) is 0.047, a relatively high value, indicating the weak protection ability of soil from vegetation.

In CSLE, the E factor refers to the changes in topography to reduce runoff and soil loss by engineering construction. Since the investigation of soil conservation measures in PSU (Figure 5e) was the major task in the Fourth National Soil Erosion Survey in China, in this study, we integrated all 117 PSU data in Zhaotong, with a grassland distribution map identified to form raster layers of the E factor using nearest-neighbor interpolation methods, and about 90% of the grassland in Zhaotong has no erosion control measures. The scarce and existing engineering measures are sloping terrace and level terrace in this region, due to the sloping land conversion program (SLCP) conducted in China.

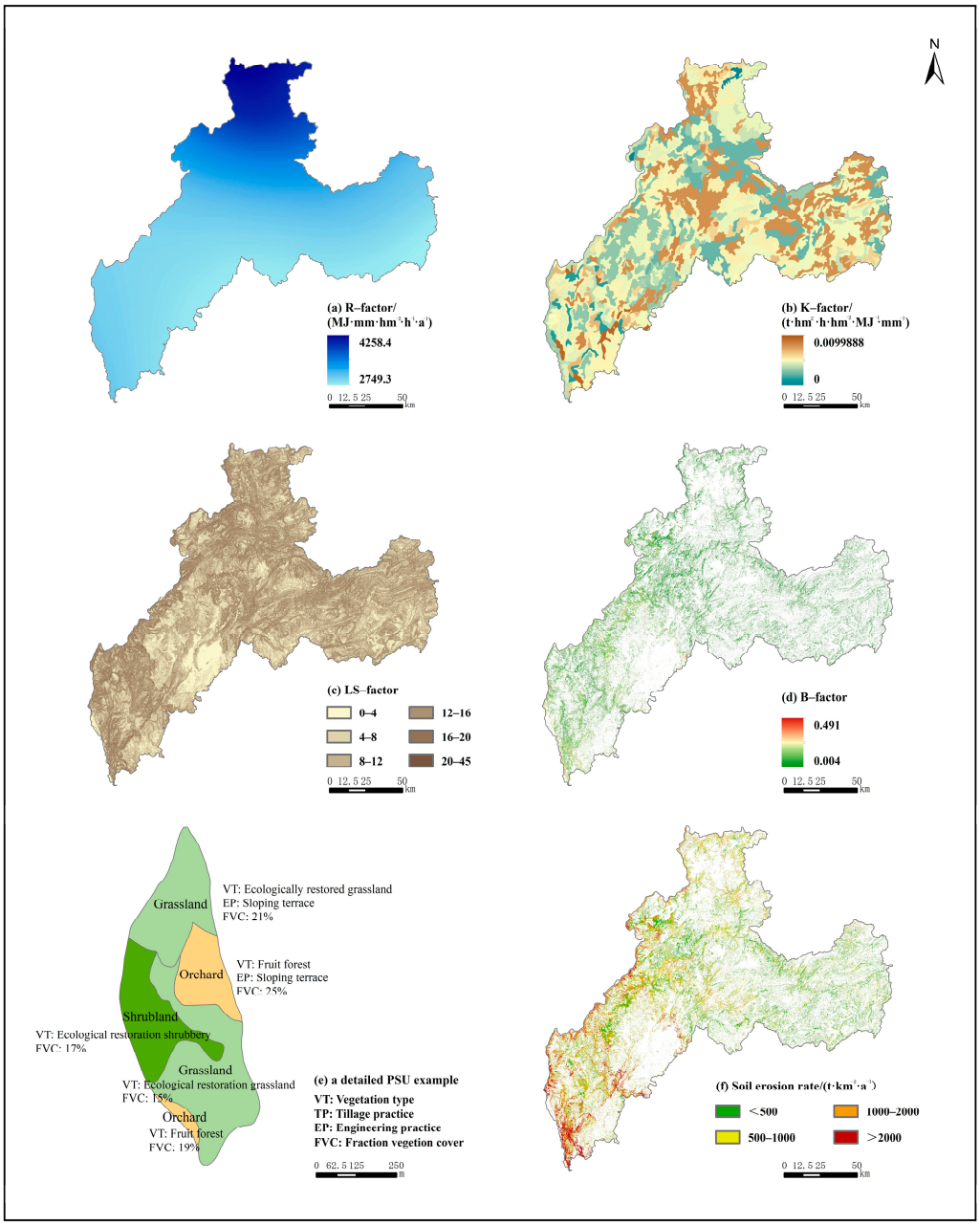

Figure 5. Quantification of grassland erosion in Zhaotong using the CSLE model: (**a**) Rainfall erosivity; (**b**) Soil erodibility; (**c**) Topographic factor; (**d**) Biological factor; (**e**) Example of field investigation units (PSUs) showing engineering and tillage measures; and (**f**) Annual average grassland erosion rate.

3.2.2. Spatial Distribution of Grassland Erosion in Zhaotong

The spatial pattern of grassland erosion in Zhaotong was revealed with the relevant factors of the CSLE model modified as input layers under a GIS framework (Figure 5f). The soil erosion rate was further classified into six grades based on SL190–2007: Standard for Classification and Gradation of Soil Erosion proposed by the Ministry of Water Resources of China. Results showed that the grassland area is suffering from water erosion with a rate greater than the tolerance (T) of 500 t/(km^2·a), accounting for 59.54% of the total grassland area. The average annual grassland erosion rate is 952.17 t/(km^2·a) and the total annual soil loss is about 5.19 × 10^6 t. As can be seen in Table 4, areas with soil erosion intensity grades higher than slight erosion only take up 8.25% of the total grassland area, but contribute to more than 30% of the total soil loss from grassland.

Table 4. Statistics of soil erosion intensity grades of grassland in Zhaotong.

Erosion Intensity	Area (km^2)	AP	SL (10^4 t)	SLP
Tolerant	2076.47	40.46%	59.83	11.53%
Slight	2631.77	51.29%	291.84	56.24%
Moderate	350.98	6.84%	116.54	22.46%
Intensive	56.39	1.10%	34.29	6.61%
Extremely intensive	15.35	0.30%	15.20	2.93%
Severe	0.71	0.01%	1.20	0.23%

AP, area percentage; SL, soil loss; SLP, soil loss percentage.

Soil erosion intensity in the grassland areas varies widely in space, and a serious erosion problem exists. On the whole, the proportion of soil loss is high in the west and low in the east. Severe and extreme erosion mainly occurred in the dry–hot valley of Jinsha River with the lowest vegetation coverage. The counties of Qiaojia and Ludian in this region even have a grassland erosion ratio (percentage of area eroded with a higher rate than soil loss tolerance in the total land) greater than 80%, while for Weixin and Zhenxiong in the east, there is almost no soil erosion occurring in the grassland.

Statistics on soil erosion in various elevation and slope zones are shown in Tables 5 and 6. It is evident that the study of grassland erosion exhibits strong vertical zonation characteristics and shows a close relationship with both the elevation and slope gradients. Grasslands within the elevation range of 800–1600 m contribute to the total soil loss the most due to the large grassland area. It should be noted that areas with an elevation above 2400 m also contribute to the erosion volume significantly, and the area of serious erosion grades (intensive and severe) and grassland erosion ratio is positively correlated with the slope. Soil erosion of the grassland in Zhaotong mostly occurs in middle- and low-elevation areas where human activities are frequent, as well as riversides, ditch sides and steep slopes, where vegetation cover is relatively low.

Table 5. Soil erosion intensity grades of grasslands for different elevation zones.

Elevation (m)	Grassland Area (km^2)						ER	SL (10^4 t)	SLP
	Tolerant	Slight	Moderate	Intensive	Extremely Intensive	Severe			
<800	181.47	273.29	30.97	7.39	3.14	0.21	63.45%	53.27	10.34%
800–1200	358.01	467.84	72.19	10.54	3.80	0.21	60.77%	98.31	19.07%
1200–1600	499.50	476.44	68.54	11.08	2.81	0.13	52.81%	99.33	19.27%
1600–2000	478.89	399.93	63.71	10.83	2.38	0.10	49.90%	87.32	16.94%
2000–2400	285.91	420.01	54.60	9.12	2.11	0.05	62.96%	80.24	15.57%
>2400	265.83	585.70	57.57	6.08	0.80	0.01	70.98%	96.91	18.80%

ER, erosion ratio; SL, soil loss; SLP, soil loss percentage.

Table 6. Soil erosion status of grasslands between different slope zones.

Slope (°)	Grassland Area (km^2)						ER	SL (10^4 t)	SLP
	Tolerant	Slight	Moderate	Intensive	Extremely Intensive	Severe			
<10	326.51	84.79	3.06	0.38	0.07	0.00	21.29%	15.04	2.91%
10–20	657.52	570.88	41.11	5.66	1.21	0.03	48.49%	94.34	18.27%
20–30	541.58	784.79	90.33	13.56	3.43	0.11	62.23%	145.05	28.09%
30–40	327.91	647.47	100.91	16.06	4.46	0.19	70.11%	133.58	25.87%
40–50	159.83	367.96	72.27	12.08	3.48	0.17	74.04%	84.36	16.34%
>50	54.88	167.46	41.03	7.77	2.61	0.21	79.97%	43.98	8.52%

ER, erosion ratio; SL, soil loss; SLP, soil loss percentage.

3.2.3. Interaction between Rainfall and Vegetation Coverage, and Its Impact on Erosion

Despite the fact that studies of regional-scale soil erosion have been reported worldwide, little is known for soil erosion rates within the year at the regional scale, especially in mountainous regions, due to the data availability of empirical models. Since mountainous areas such as Zhaotong are more sensitive to monsoons and climate change, it is definitely essential to understand the temporal erosion conditions to support the selection of when to conduct restoration efforts. Thus, we analyzed the temporal distribution of R, FVC and corresponding grassland erosion across the year to reflect the interaction between rainfall and grassland vegetation coverage.

In order to intuitively reflect the interaction relationship between precipitation and vegetation, the monthly precipitation distribution in Zhaotong, which was extracted from meteorological satellite data for calculating the annual R value, is shown in Figure 6. Obviously, grassland erosion is significantly impacted by the interaction and variation between rainfall and vegetation. As the uneven distribution of rainfall in time and space, the distribution of the R factor, FVC and soil erosion is also extremely uneven across the year, and all of them show a trend of increasing first and then decreasing, reaching the maximum in July, August and June, respectively (Table 7). Grassland erosion from May to October occupied 93.32% of the total soil loss of the year because of abundant precipitation. Although vegetation cover is one of the major affecting factors of grassland erosion, soil erosion is not serious from December to April, when the vegetation cover is the lowest during the year. This is because the R factor during this period only accounts for 2.6% of the year and lacks the key factors that trigger soil erosion. Nevertheless, low vegetation coverage caused by climate change is the dominant factor causing grassland erosion.

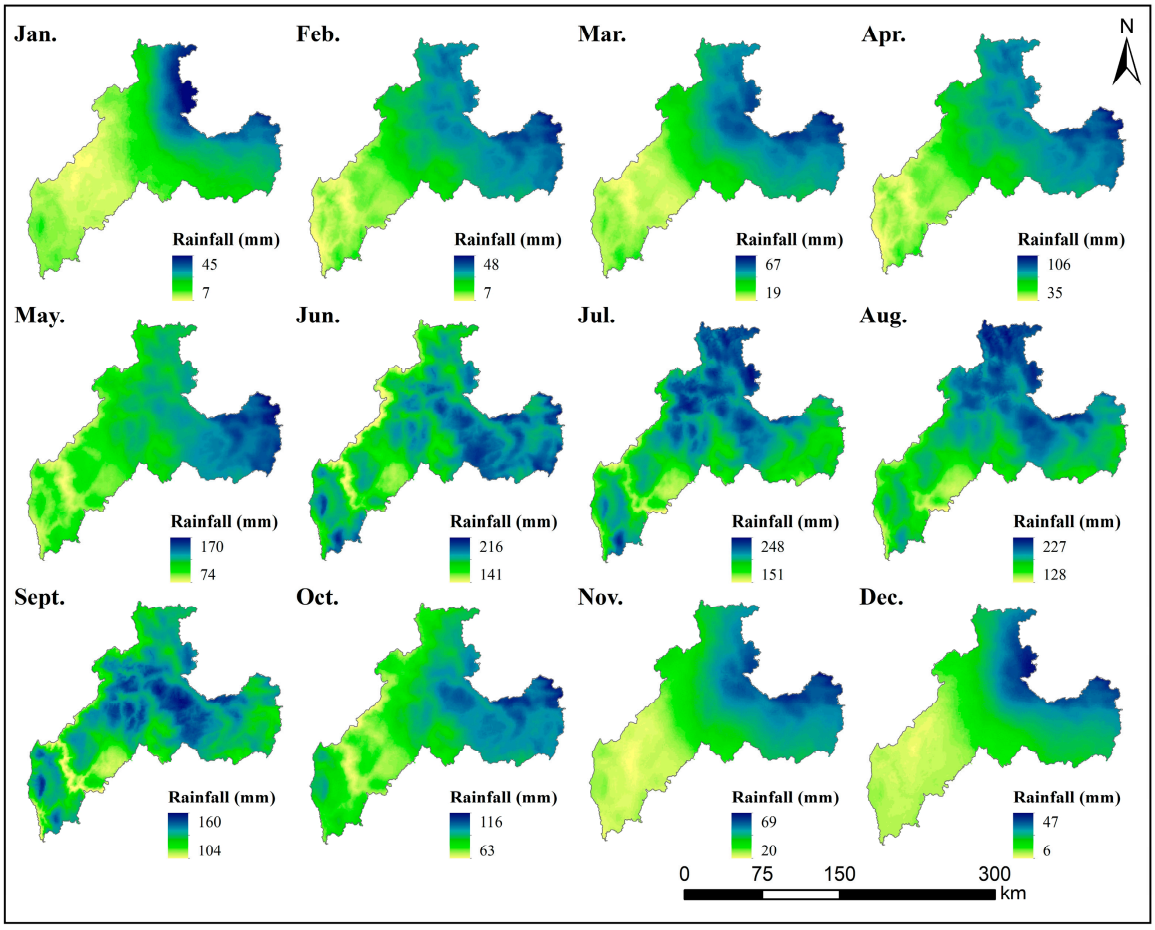

Figure 6. Average monthly rainfall distribution in Zhaotong from 2000 to 2020.

Table 7. Distribution of R, FVC and corresponding grassland soil erosion across the year.

Month	January	February	March	April	May	June	July	August	September	October	Novermber	December
R	0.11%	0.17%	0.54%	1.78%	6.00%	22.10%	29.33%	25.25%	9.54%	4.75%	0.43%	0
FVC	42.13%	40.71%	38.85%	48.48%	49.78%	58.00%	68.96%	72.80%	70.35%	69.57%	56.71%	48.81%
Soil Erosion	0.29%	0.47%	1.59%	3.84%	12.59%	35.23%	21.76%	14.15%	6.44%	3.15%	0.49%	0

With the arrival of the rainy season, the vegetation coverage of the grassland also increases. However, the lag effect of grassland vegetation protection on soil is obvious, especially in dry–hot valleys. Specifically, the most soil erosion occurred in June, but not the months after it with higher vegetation coverage or R values, which indicates that the start of the rainy season is the most critical stage for erosion control and ecological restoration efforts.

3.3. Grassland Regrowth Rate and Restoration Potential

Regrowth rate refers to the speed of grassland restoration, and is defined as the per–centage of the grass yield that continues to grow after grazing or mowing, when the aboveground biomass of grasslands reaches the highest level. According to the agricultural industry standard of China "calculation of reasonable carrying capacity of natural grassland" (NY/T 635–2015), the grassland in Zhaotong was further divided into four classes based on elevation: thermal grassland, warm–temperate grassland, temperate grassland and alpine grassland [74]. The corresponding regrowth rates of each grassland type were 30%, 20%, 15% and 5%, respectively. Figure 7b illustrates the general grassland regeneration pattern, being high in the north and low in the south, and there are obvious vertical zonal distribution characteristics. The regrowth rate is higher than 20% in most areas; in other words, as long as the proper ecological restoration measures and conservation policies are put in place, most areas can return to a much better situation in a relatively short period of time.

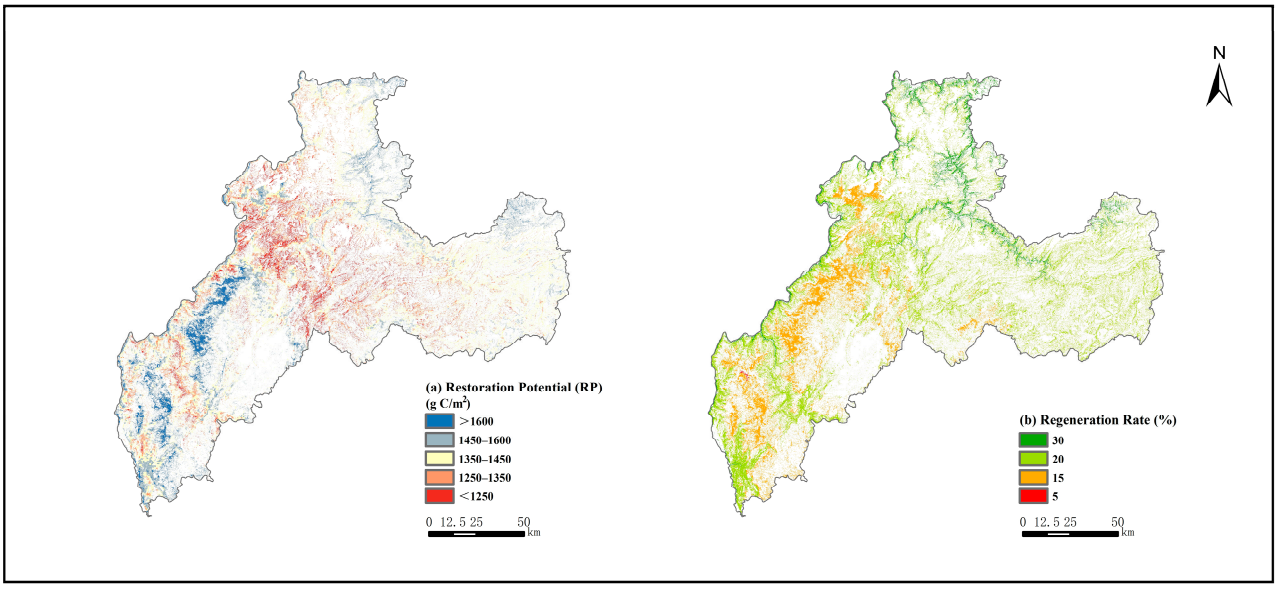

Figure 7. (**a**) Maps of grassland restoration potential (**b**) and grassland regrowth rate in Zhaotong.

The distribution map of estimated grassland RP in Zhaotong is shown in Figure 7a. Vegetation restoration potential represents the gap between the actual vegetation growth and the ideal statue. To some extent, it also indicates the degree of ecosystem degradation; that is, the greater the RP value, the greater the degradation degree. Apparently, the grassland RP is roughly increasing from northeast to southwest, which is similar to the soil erosion distribution pattern. Grasslands with low RP values are mainly distributed in

the elevation range of 800–2100 m (warm grassland). The grassland RP of zones with an elevation above 2100 m is generally higher, which indicates that human activities are not the major driver of grassland degradation, since most of the population is distributed in the 800–2100 m zone with a fine vegetation cover. Additionally, as the slope rises, the potential of grassland restoration improves. It should be noted that more than 60% of the grassland has an RP value greater than 1350 g C/m^2, indicating an overall promising performance of grassland vegetation restoration.

Figure 8 was drawn based on the RP values during 2000–2020. It depicts the interannual RP trend of each type of grassland in Zhaotong. The analysis showed that alpine grassland was a grassland type with a high RP value, ranging from 1226.92 to 1851.86 g C/m^2, and the fluctuation was relatively higher than other types of grassland. However, this type of grassland accounts for the smallest proportion of Zhaotong grassland. In contrast, the warm grassland with the largest area proportion has the lowest recovery potential, ranging from 765.37 to 1338.02 g C/m^2. The low and non-significant interannual fluctuation RP of warm grasslands makes the restoration value of this type of grassland lower, which also indicates that its degradation degree is lower. In addition, thermal and temperate grasslands with more serious soil erosion also have higher RP values, ranging from 910.30 to 1420.12 g C/m^2 and 851.93 to 1560.47 g C/m^2, respectively. We found that the overall trend of the restoration potential of the four types of typical grasslands showed large fluctuation. The underlying reasons include the frequent occurrence of climate change, such as extreme precipitation and drought, the inconsistent protection focus of the decision-making departments each year and the continuous change in the scale of grazing.

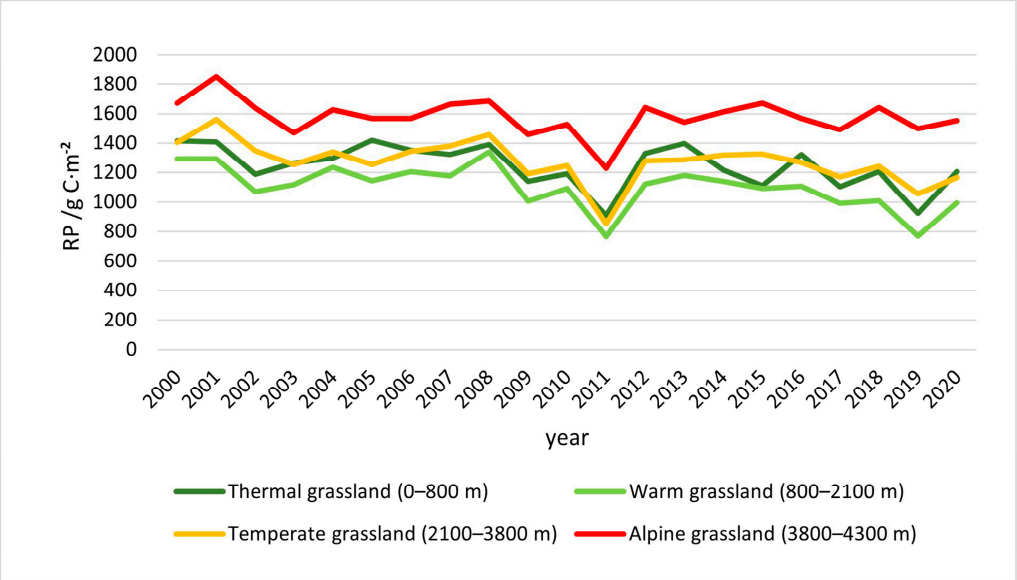

Figure 8. Interannual RP trends of the four typical grassland types.

3.4. Grassland Restoration Patterns

Table 8 displays the zoning descriptions and results of the spatial overlay analysis, and Figure 9 displays the divisions and distribution of the grassland restoration patterns. The results show that most Class A and Class C grasslands that do not require artificial intervention are located below 2000 m in elevation, and are primarily thermal and warm–temperate grasslands with high regeneration rates. Grasslands of Class E and Class G, with high regeneration rates but serious soil erosion, are widely distributed in steep slope areas, with high grazing intensity and serious degradation. Among them, Class E grasslands have a higher restoration potential and grazing value, so they should be the focus of closure and protection. Most Class B, D, F and H grasslands with lower regeneration rates are located in the southwestern part of Zhaotong, at a higher elevation range, and are

mostly subalpine meadows with higher utilization rates. Among them, Class B and Class D grasslands with less serious soil erosion are sparse in area distribution, and most of them are characterized with low regeneration rates and serious soil erosion. This type of grassland can be represented by the alpine grassland in the Yaoshan Nature Reserve of Qiaojia County, which has a high protein content for grazing, and is currently degraded due to the increase in livestock. Therefore, the primary focus should be protecting the natural grasslands, cultivation and adopting various human interventions to achieve the ideal ecological structure.

Table 8. Description of treatment for each grassland region and restoration patterns.

Region	Area (km^2) and Percentage	Restoration Patterns
A	343.95 (8.95%)	High RP–High RR–Tolerant SE, achieve better restoration results without artificial promotion and special measures, natural repair.
B	242.21 (6.30%)	High RP–Low RR–Tolerant SE, demand a longer closure protection time cycle for restoration.
C	770.86 (20.05%)	Low RP–High RR–Tolerant SE, with better quality grass and less space for restoration, grazing according to topography and climate.
D	108.41 (2.82%)	Low RP–Low RR–Tolerant SE, mowing and grazing while cultivating and improving grassland.
E	664.91 (17.29%)	High RP–High RR–Serious SE, unsustainable, methods, such as slope sealing and grass cultivation, moderate grazing, etc., should be adopted to restore its ecological function.
F	653.21 (16.99%)	High RP–Low RR–Serious SE, unsustainable, demand multifaceted human intervention to achieve the desired ecological structure.
G	890.07 (23.15%)	Low RP–High RR–Serious SE, unsustainable, protection should be the main focus to strengthen vegetation restoration.
H	171.25 (4.45%)	Low RP–Low RR–Serious SE, unsustainable, demand urgent human intervention, adopt active soil conservation measures, such as fence sealing and artificial grass planting, to promote soil nutrients and productivity.

RP, restoration potential; RR, regrowth rate; SE, soil erosion.

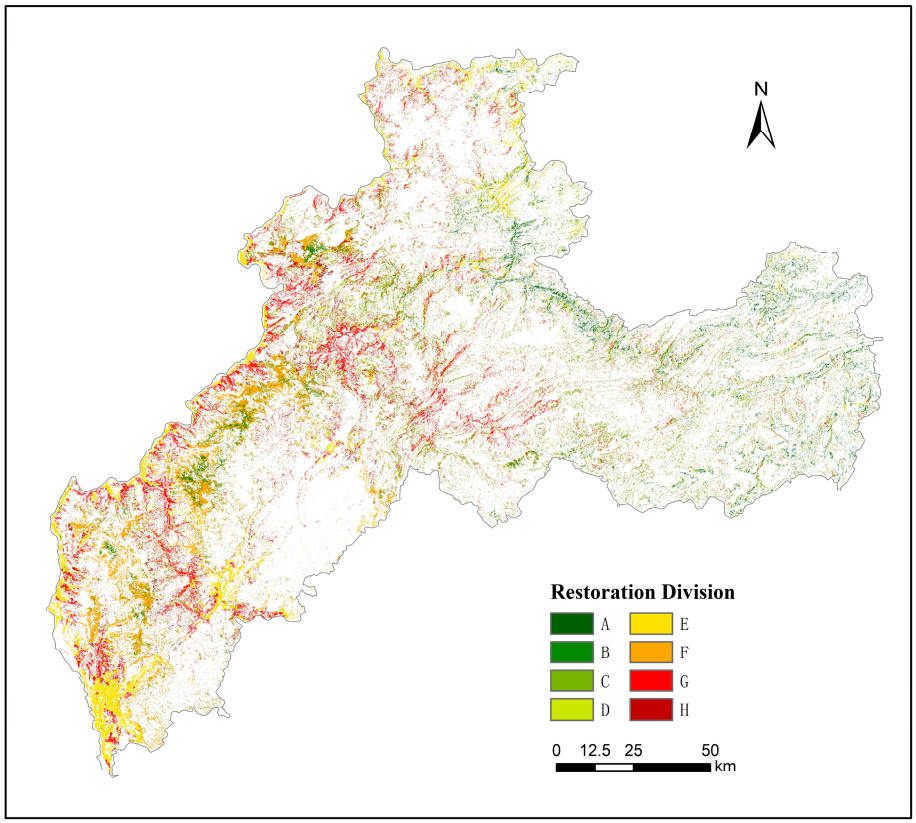

Figure 9. Division and distribution of grassland restoration pattern in Zhaotong.

4. Discussion

4.1. Quantitative Assessment of the Grassland Restoration Patterns

Despite the fact that the importance of grassland ecosystems and the socio-ecological environmental implications of grassland degradation have been well recognized, grassland restoration is still not being taken seriously. Therefore, we try to establish an erosion-based approach to achieve the goal of regional or large-scale grassland restoration by integrating the drivers, results, potential and recovery speed of grassland. However, other perspectives, such as biodiversity and ecosystem service should also be considered in the future. With the demand for precise governance in China, a quantitative restoration guide is of the utmost importance for policy makers.

Although previous studies have assessed grassland restoration using satellite imagery, and demonstrated that soil erosion is the main cause of grassland degradation in Southern China, rather than over-grazing. These studies merely classified the grassland restoration patterns and constructed spatial distribution maps. Quantitative assessments of the factors that determine grassland restoration at large spatio-temporal scales are lacking in China. Located in the one of the National Key Management Areas of Soil Erosion in China, the erosion-based restoration modes in Zhaotong are consistent with the survey results of the China Soil and Water Conservation Bulletin, but with a higher time resolution of 10 m and continuous grassland cover. We also achieved grassland soil erosion quantitative estimation at the regional scale, which makes our work different from the previous soil erosion studies.

The fragmented distribution and complex natural environment of grasslands in southern China generally result in poor identification accuracy. Based on multi-source remote sensing data, the non-homogenous data voting and random forest classification method are used to identify grassland distribution, which provides a higher classification accuracy compared to existing available LULC datasets, and proves to be more effective and efficient in identifying fragmented grasslands in mountainous and hilly regions. However, in terms of input feature selection and time series vegetation cover construction, visual estimation was also employed. Due to the knowledge differences between different investigators, manual subjectivity is inevitable, which will affect the classification results to some extent.

The regeneration rate is calculated based on local government statistics and standards, which varies greatly from year to year. This can only be used as a relative reference threshold and uncertainties exist in the evaluation process. We did analyze the interaction of rainfall–soil–plant system, but with the increase of global extreme climate events which generate large amounts of soil erosion, the amount of soil erosion produced by a single extreme rainfall event may exceed the annual values, this is not considered in this study.

4.2. Uncertainties

A high interannual variation in grassland RP was also found in Zhaotong. This is mainly because temperature and precipitation are the only driving parameters in NPP estimation, and the establishment of NPP estimation model is affected by human factors, data quality, model parameter values, grassland vegetation types and geographical location. Thus, there are still differences in estimation results among different products in the same area and location. There are also issues of misclassification and omission with the land-use/cover data products used in the study. Methods of obtaining high-precision land-use/cover data for complex terrains in southwestern China demand further discussion and study. It should be noted that the establishment of the CSLE model is to estimate long-term average sheet and rill erosion from a single slope, other erosion types are not included, which will also lead to serious grassland degradation. Additionally, despite the CSLE model having been well studied and widely applied for different landscapes in China, previous runoff plots were mostly concentrated on cultivated land, and further grassland plot experiments are also needed for this region to verify our erosion estimation results.

4.3. Future Challenges

Relevant research has evaluated grassland restoration in northern China using the StageTHREE Sustainable Grassland model (StageTHREE SGM), which integrates the dynamics of grassland and soil resources, wind erosion, livestock production and herder household economics to provide a useful tool for finding sustainable solutions for grassland systems. Due to the difference in the drivers of grassland restoration, especially the difference in scale, the uncertainty of data, model and scale effects will be caused. Different stakeholders and different scales of research have a different understanding of restoration. This paper presents a simple and rapid evaluation method for degraded grassland in southwest mountainous areas. Its biggest advantage compared to other studies is that it combines field survey data to supplement the characteristics of the special environment in the mountainous area. Considering the conflict between the restoration goals at multiple scales, restoration actions need to counteract local-scale habitat degradation, as well as sustaining natural migration across landscapes. Restoration scientists and practitioners should be called upon to face grassland restoration challenges at various scales.

5. Conclusions

Given the extent of global land degradation resulting from climate changes and human activities, restoration efforts have been increasingly focused on grassland conservation schemes to ensure the long-term sustainability of biodiversity and ecosystem services. Quantitative restoration assessment is one of the most important scientific foundations for land resource management. Apparently, a satellite remote sensing approach is likely to be a significant contributor to support conservation strategies by providing relevant spatio-temporal information. While there are many experimental studies and qualitative reports about the causes, consequences and processes of grassland restoration from different perspectives and with various indicators, grasslands are still under a major threat from ongoing degradation, since little progress has been made in finding standardized soci—ecological solutions to reverse degradation.

This study describes a new approach for zoning mountainous grassland restoration, using multi-source remote sensing data. We emphasize that caution is warranted when choosing grassland restoration modes, and that long-term sustainability of grassland can be achieved only when multiple factors of both the above-ground vegetation and soil conditions are considered. Based on both optical and SAR sensors, regional scale identification of grassland distribution was completed in Zhaotong using a random forest classification method. A fine quantification of grassland erosion using the CSLE model was achieved. The grassland restoration potential in the research region was further estimated by calculating the gap between ANPP and PNPP. The grassland regrowth rate was obtained and then overlaid to provide a basis for supporting conservation schemes.

The method proposed for remote sensing grassland identification, using non-homologous data voting, has an overall accuracy of 88.21%, which can meet the requirements of a regional-scale study. The findings indicate that the grassland restoration potential in Zhaotong is generally performing well. Low values are primarily found in the 800–2100 m range with intensive human activity, and the overall trend for restoration potential has been steadily declining during the last two decades. The average soil erosion rate of grassland is 952.17 t/(km^2·a), and about 60% of the grasslands are showing unaccepted erosion rates. Furthermore, the interaction between rainfall and vegetation suggests that in large geographical extents, restoration conditions and solutions can significantly vary, both in time and space, and the low vegetation cover and precipitation change, rather than human activities, accelerates the degradation of grassland in the region. Our results also suggest that grassland restoration can be effective only when different grasslands are treated with various management strategies, and those in severely degraded conditions with low regrowth rates, in the southwest dry–hot valley, are calling for human intervention immediately.

We argue that urgent action is needed to face the process and challenges of grassland degradation, as well as the increasing recognition in policies and regulations. To restore

grassland sustainability, shared understanding, developed standardized indicators and data sharing regarding restoration experiences by different roles, stakeholders, collaborations and mutual relationships are also needed.

Author Contributions: Conceptualization, methodology and funding acquisition, G.C.; conducted the experiments and wrote the manuscript, Y.W.; G.C., Q.W. and L.Z., review and editing this paper, G.C., Q.W. and L.Z.; contributed extensively to data processing and formal analysis, J.Z. All authors have read and agreed to the published version of the manuscript.

Funding: This research was supported by Yunnan Fundamental Research Projects (Grant No. 202101AU070161) and the Strategic Priority Research Program of Chinese Academy of Sciences (Grant No. XDA26050301–01).

Data Availability Statement: Not applicable.

Acknowledgments: Thanks to the field data gatherers in the National Soil Erosion Survey for their invaluable efforts.

Conflicts of Interest: The authors declare no conflict of interest.

References

1. Suttie, J.M.; Reynolds, S.G.; Batello, C. *Grasslands of the World*; Food and Agriculture Organization of the United Nations: Rome, Italy, 2005.
2. Dengler, J.; Janišová, M.; Török, P.; Wellstein, C. Biodiversity of Palaearctic grasslands: A synthesis. *Agric. Ecosyst. Environ.* **2014**, *182*, 1–14. [CrossRef]
3. Sun, J.; Wang, Y.; Piao, S.; Liu, M.; Han, G.; Li, J.; Liang, E.; Lee, T.M.; Liu, G.; Wilkes, A.; et al. Toward a sustainable grassland ecosystem worldwide. *Innovation* **2022**, *3*, 100265. [CrossRef] [PubMed]
4. Zhao, Y.; Liu, Z.; Wu, J. Grassland ecosystem services: A systematic review of research advances and future directions. *Landsc. Ecol.* **2020**, *35*, 793–814. [CrossRef]
5. Abberton, M.; Conant, R.; Batello, C. *Grassland Carbon Sequestration: Management, Policy and Economics*; Food and Agriculture Organization of the United Nations: Rome, Italy, 2010.
6. Gibbs, H.K.; Salmon, J.M. Mapping the world's degraded lands. *Appl. Geogr.* **2005**, *57*, 12–21. [CrossRef]
7. Török, P.; Brudvig, L.A.; Kollmann, J.; N Price, J.; Tóthmérész, B. The present and future of grassland restoration. *Restor. Ecol.* **2021**, *29*, e13378. [CrossRef]
8. Gang, C.; Zhou, W.; Chen, Y.; Wang, Z.; Sun, Z.; Li, J.; Qi, J.G.; Odeh, I. Quantitative assessment of the contributions of climate change and human activities on global grassland degradation. *Environ. Earth Sci.* **2014**, *72*, 4273–4282. [CrossRef]
9. Bardgett, R.D.; Bullock, J.M.; Lavorel, S.; Manning, P.; Schaffner, U.; Ostle, N.; Chomel, M.; Durigan, G.; Fry, E.L.; Johnson, D.; et al. Combatting global grassland degradation. *Nat. Rev. Earth Environ.* **2021**, *2*, 720–735. [CrossRef]
10. Ren, J.Z. Current condition and productive potential of grasslands in southern China. *Acta Pratacult. Sin.* **1999**, *8*, 23–31. (In Chinese)
11. Wang, Z.; Ma, Y.; Zhang, Y.; Shang, J. Review of remote sensing applications in grassland monitoring. *Remote Sens.* **2022**, *14*, 2903. [CrossRef]
12. Pettorelli, N.; Schulte to Bühne, H.; Tulloch, A.; Dubois, G.; Macinnis-Ng, C.; Queirós, A.M.; Keith, D.A.; Wegmann, M.; Schrodt, F.; Stellmes, M.; et al. Satellite remote sensing of ecosystem functions: Opportunities, challenges and way forward. *Remote Sens. Ecol. Conserv.* **2018**, *4*, 71–93. [CrossRef]
13. Ali, I.; Cawkwell, F.; Dwyer, E.; Barrett, B.; Green, S. Satellite remote sensing of grasslands: From observation to management. *J. Plant Ecol.* **2016**, *9*, 649–671. [CrossRef]
14. Becker, A.; Bugmann, H. Global change and mountain regions—An IGBP initiative for collaborative research. In *Global Change and Protected Areas*; Visconti, G., Beniston, M., Iannorelli, E.D., Barba, D., Eds.; Advance in Global Change Research: Laquila, Italy, 2001.
15. Kräuchi, N.; Brang, P.; Schönenberger, W. Forests of mountainous regions: Gaps in knowledge and research needs. *For. Ecol. Manag.* **2000**, *132*, 73–82. [CrossRef]
16. Andrade, B.O.; Koch, C.; Boldrini, I.I.; Vélez–Martin, E.; Hasenack, H.; Hermann, J.M.; Kollmann, J.; Pillar, V.D.; Overbeck, G.E. Grassland degradation and restoration: A conceptual framework of stages and thresholds illustrated by southern Brazilian grasslands. *Nat. Conserv.* **2015**, *13*, 95–104. [CrossRef]
17. Akiyama, T.; Kawamura, K. Grassland degradation in China: Methods of monitoring, management and restoration. *Grassl. Sci.* **2007**, *53*, 1–17. [CrossRef]

18. Cheng, X.; Liu, W.; Zhou, J.; Wang, Z.; Zhang, S.; Liao, S. Extraction of mountain grasslands in yunnan, china, from sentinel–2 data during the optimal phenological period using feature optimization. *Agronomy* **2022**, *12*, 1948. [CrossRef]
19. Li, Y.C.; Ge, J.; Hou, M.J.; Gao, H.Y.; Liu, J.; Bao, X.Y.; Yin, J.P.; Gao, J.L.; Feng, Q.S.; Liang, T.G. A study of the spatiotemporal dynamic of land cover types and driving forces of grassland area change in Gannan Prefecture and Northwest Sichuan based on CCI–LC data. *Acta Pratacult. Sin.* **2020**, *29*, 1–15. (In Chinese)
20. Li, J.; Wen, G.; Li, D. Application of multi–source remote sensing image in yunnan province grassland resources investigation. *Int. Arch. Photogram. Remote Sens. Spatial Inform. Sci.* **2018**, *42*, 837–841. [CrossRef]
21. Pan, H.T.; Wang, X.; Wang, X.F. Study on the effect of training samples on the accuracy of crop remote sensing classification. *Infrared Laser Eng.* **2017**, *46*, 149–156. (In Chinese)
22. Tang, J.; Alelyani, S.; Liu, H. Feature selection for classification: A review. In *Data Classification, Algorithms and Applications*; Routledge: New York, NY, USA, 2014.
23. Kwak, N.; Choi, C.H. Input feature selection for classification problems. *IEEE Trans. Neural Netw.* **2002**, *13*, 143–159. [CrossRef]
24. Zhang, H.; Shi, W.Z.; Wang, Y.J. *Study on Reliable Classification Methods Based on Remotely Sensed Image*; Surveying and Mapping Press: Beijing, China, 2006.
25. Zhang, M.; Qian, Y.R.; Du, J.; Fan, Y.Y. The application of the convolution neural network to grassland classification in remote sensing images. *J. Northeast Norm. Univ. Nat. Sci. Ed.* **2019**, *51*, 53–58. (In Chinese)
26. Senf, C.; Leitão, P.J.; Pflugmacher, D.; Linden, S.V.D.; Hostert, P. Mapping land cover in complex mediterranean landscapes using Landsat: Improved classification accuracies from integrating multi–seasonal and synthetic imagery. *Remote Sens. Environ.* **2015**, *156*, 527–536. [CrossRef]
27. Liu, C.L.; Hsaio, W.H.; Tu, Y.C. Time series classification with multivariate convolutional neural network. *IEEE Trans. Ind. Electron.* **2018**, *66*, 4788–4797. [CrossRef]
28. Hatami, N.; Gavet, Y.; Debayle, J. Classification of time–series images using deep convolutional neural networks. In Proceedings of the Tenth International Conference on Machine Vision, Vienna, Austria, 13–15 November 2018; pp. 242–249.
29. Zhao, L.C.; Liu, R.T.; Yang, Y.H.; Li, Y.J.; Zhang, X.Q.; Sun, X.L. Study on the remote sensing classification of grasslands based on the topographic factors. *Pratacult. Sci.* **2006**, *23*, 26–30. (In Chinese)
30. Yang, Z.S.; Liang, L.H. Soil erosion under different land use types and zones of Jinsha River Basin in Yunnan Province, China. *J. Mt. Sci.* **2004**, *1*, 46–56.
31. Wischmeier, W.H.; Smith, D.D. *Predicting Rainfall–Erosion Losses from Cropland East of the Rocky Mountains: Guide for Selection of Practices for Soil and Water Conservation*; US Government Printing Office: Washington, DC, USA, 1978; p. 33.
32. Renard, K.G.; Foster, G.R.; Weesies, G.A.; McCool, D.K.; Yoder, D.C. *Predicting Soil Erosion by Water: A Guide to Conservation Planning with the Revised Universal Soil Loss Equation (RUSLE)*; US Government Printing Office: Washington, DC, USA, 1997; p. 301.
33. Liu, B.Y.; Zhang, K.L.; Xie, Y. An Empirical Soil Loss Equation. In Proceedings of the 12th ISCO Conference, Beijing, China, 26–31 May 2002; p. 143.
34. Xie, Y.; Yue, T.Y. Application of soil erosion models for soil and water conservation. *Sci. Soil Water Conserv.* **2018**, *16*, 25–37. (In Chinese)
35. Alewell, C.; Borrelli, P.; Meusburger, K.; Panagos, P. Using the USLE: Chances, challenges and limitations of soil erosion modelling. *Int. Soil Water Conserv. Res.* **2019**, *7*, 203–225. [CrossRef]
36. Duan, X.; Bai, Z.; Rong, L.; Li, Y.; Ding, J.; Tao, Y.; Li, J.; Wang, W. Investigation method for regional soil erosion based on the Chinese Soil Loss Equation and high–resolution spatial data: Case study on the mountainous Yunnan Province, China. *Catena* **2020**, *184*, 104237. [CrossRef]
37. Feng, J.X.; Chen, G.K.; Zuo, L.J.; Wen, Q.K.; Zhao, J.J.; Wang, Y.W. Quantitative evaluation and characteristic analysis of cultivated land erosion in mountain area using GF–6 WFV and CSLE model. *Trans. CSAE* **2022**, *38*, 169–179. (In Chinese)
38. Liu, Y.; Zhang, Z.; Tong, L.; Khalifa, M.; Wang, Q.; Gang, C.; Wang, Z.; Li, J.; Sun, Z. Assessing the effects of climate variation and human activities on grassland degradation and restoration across the globe. *Ecol. Indic.* **2019**, *106*, 105504. [CrossRef]
39. Wang, Y.; Ren, Z.; Ma, P.; Wang, Z.; Niu, D.; Fu, H.; Elser, J.J. Effects of grassland degradation on ecological stoichiometry of soil ecosystems on the Qinghai–Tibet Plateau. *Sci. Total Environ.* **2020**, *722*, 137910. [CrossRef]
40. Laughlin, D.C. Applying trait–based models to achieve functional targets for theory–driven ecological restoration. *Ecol. Lett.* **2014**, *17*, 771–784. [CrossRef]
41. Wang, R.J.; Feng, Q.S.; Jin, Z.R.; Liu, J.; Zhao, Y.T.; Ge, J.; Liang, T.G. A study on restoration potential of degraded grassland on the Qinghai–Tibetan Plateau. *Acta Pratacult. Sin.* **2022**, *31*, 11–22. (In Chinese)
42. Wang, K.L.; Wang, Z.H.; Xiao, P.Q.; Wang, T.S.; Zhang, P. Evaluation of restoration potential of shrubs–herbs–arbor vegetation coverage on the Loess Plateau based on the principle of water balance. *Acta Ecol. Sin.* **2022**, *42*, 8352–8364. (In Chinese)
43. Reinermann, S.; Asam, S.; Kuenzer, C. Remote sensing of grassland production and management—A review. *Remote Sens.* **2020**, *12*, 1949. [CrossRef]
44. Zhang, R.; Liang, T.; Guo, J.; Xie, H.; Feng, Q.; Aimaiti, Y. Grassland dynamics in response to climate change and human activities in Xinjiang from 2000 to 2014. *Sci. Rep.* **2018**, *8*, 2888. [CrossRef]

45. Zhou, W.; Gang, C.; Zhou, F.; Li, J.; Dong, X.; Zhao, C. Quantitative assessment of the individual contribution of climate and human factors to desertification in northwest China using net primary productivity as an indicator. *Ecol. Indic.* **2015**, *48*, 560–569. [CrossRef]
46. Li, Q.; Gao, S.; Zhang, C.; Wang, R.; Zhou, N.; Li, J.; Guo, Z.; Chang, C. Assessment of the impacts of climate change and human activities on the dynamic grassland change in Inner Mongolia. *Geogr. Geo-Inf. Sci.* **2019**, *35*, 99–104.
47. Terwayet, B.O.; Zhang, W.; Terwayet, B.H. Assessment of drought characteristics and its impacts on net primary productivity (NPP) in southeastern Tunisia. *Arab. J. Geosci.* **2023**, *16*, 26. [CrossRef]
48. Ghorbani, A.; Arzani, H.; Azizi, M.J.; Mostafazadeh, R. Modelling Above ground net primary production of Sabalan rangelands using vegetation index and non-linear regression. *Rangeland* **2022**, *16*, 33–51.
49. Baeza, S.; Lezama, F.; Piñeiro, G.; Altesor, A.; Paruelo, J.M. Spatial variability of above-ground net primary production in Uruguayan grasslands: A remote sensing approach. *Appl. Veg. Sci.* **2010**, *13*, 72–85. [CrossRef]
50. Franklin, S.E.; Lavigne, M.B.; Deuling, M.J.; Wulder, M.A.; Hunt Jr, E.R. Estimation of forest leaf area index using remote sensing and GIS data for modelling net primary production. *Int. J. Remote Sens.* **1997**, *18*, 3459–3471. [CrossRef]
51. Chen, G.; Yu, C.Q.; Shen, Z.X.; Li, J.H. *Grassland Quality Monitoring*; Yunnan University Press: Kunming, China, 2018.
52. Huangfu, J.Y.; Mao, F.X.; Lu, X.S. Analysis of grassland resources in southwest China. *Acta Pratacult. Sin.* **2012**, *21*, 75–82. (In Chinese)
53. Cheng, X.B.; Yang, Z.S. Temporal and spatial variation characteristics and driving forces of land use in Zhaotong City of Yunnan Province. *Bull. Soil Water Conserv.* **2018**, *38*, 166–170. (In Chinese)
54. Rao, J.; Li, X.C. Discussion on the status quo and countermeasures of the industrialization of animal husbandry in Zhaotong City. *Contemp. Anim. Husb.* **2016**, *5*, 78–79. (In Chinese)
55. Liu, J.Y. *Remote Sensing Spatiotemporal Information of Land Use Change in China in the 1990s*; Science Press: Beijing, China, 2005; p. 26.
56. Chen, J.; Liao, A.P.; Chen, J.; Peng, S.; Chen, L.J.; Zhang, H.W. 30–meter global land cover data product–Globeland30. *Geomat. World* **2017**, *24*, 1–8.
57. Buchhorn, M.; Smets, B.; Bertels, L.; De Roo, B.; Lesiv, M.; Tsendbazar, N.E.; Li, L.; Tarko, A. *Copernicus Global Land Service: Land Cover 100m: Version 3 Globe 2015–2019: Validation Report*; Zenodo: Geneve, Switzerland, 2020.
58. Zhang, X.; Liu, L.Y.; Chen, X.D.; Gao, Y.; Xie, S.; Mi, J. GLC_FCS30: Global land–cover product with fine classification system at 30m using time–series Landsat imagery. *Earth Syst. Sci. Data* **2021**, *13*, 2753–2776. [CrossRef]
59. Gong, P.; Liu, H.; Zhang, M.N.; Li, C.C.; Wang, J.; Huang, H.B.; Clinton, N.; Ji, L.Y.; Li, W.Y.; Bai, Y.Q.; et al. Stable classification with limited sample: Transferring a 30–m resolution sample set collected in 2015 to mapping 10–m resolution global land cover in 2017. *Sci. Bull.* **2019**, *64*, 370–373. [CrossRef]
60. Su, Y.; Guo, Q.; Hu, T.; Guan, H.C.; Jin, S.C.; An, S.Z.; Chen, X.L.; Guo, K.; Hao, Z.Q.; Hu, Y.M.; et al. An updated vegetation map of China (1:1,000,000). *Sci. Bull.* **2020**, *65*, 1125–1136. [CrossRef]
61. Yuan, Y.; Wen, Q.; Zhao, X.; Liu, S.; Zhu, K.; Hu, B. Identifying grassland distribution in a mountainous region in southwest China using multi–source remote sensing images. *Remote Sens.* **2022**, *14*, 1472. [CrossRef]
62. Zhu, X.F.; Pan, Y.Z.; Zhang, J.S.; Wang, S.; Gu, X.H.; Xu, C. The Effects of training samples on the wheat planting area measure accuracy in TM scale (I): The accuracy response of different classifiers to training samples. *J. Remote Sens.* **2006**, *11*, 826–837.
63. Breiman, L. Random forests. *Mach. Learn.* **2001**, *45*, 5–32. [CrossRef]
64. Chen, G.; Zhang, Z.; Guo, Q.; Wang, X.; Wen, Q. Quantitative assessment of soil erosion based on CSLE and the 2010 national soil erosion survey at regional scale in Yunnan Province of China. *Sustainability* **2019**, *11*, 3252. [CrossRef]
65. Liu, B.; Guo, S.; Li, Z.; Xie, Y.; Zhang, K.; Liu, X. Sampling survey of water erosion in China. *Soil Water Conserv. China* **2013**, *8*, 26–34. (In Chinese)
66. Liu, B.; Xie, Y.; Li, Z.; Liang, Y.; Zhang, W.; Fu, S.; Yin, S.Q.; Wei, X.; Zhang, K.; Wang, Z.Q.; et al. The assessment of soil loss by water erosion in China. *Int. Soil Water Conserv. Res.* **2020**, *8*, 430–439. [CrossRef]
67. Chen, G.K. Quantitative Assessment and Comparision of Soil Erosion by Water Based on Field Sampling Survey Data in China. Ph.D. Thesis, University of Chinese Academy of Sciences, Beijing, China, 2019.
68. Liu, B.Y.; Nearing, M.A.; Shi, P.J.; Jia, Z.W. Slope length effects on soil loss for steep slopes. *Soil Sci. Soc. Am. J.* **2000**, *64*, 1759–1763. [CrossRef]
69. McCool, D.K.; Brown, L.C.; Foster, G.R.; Mutchler, C.K.; Meyer, L.D. Revised slope steepness factor for the universal soil loss equation. *Trans. ASAE* **1987**, *30*, 1387–1396. [CrossRef]
70. Liu, B.Y.; Nearing, M.A.; Risse, L.M. Slope gradient effects on soil loss for steep slopes. *Trans. ASAE* **1994**, *37*, 1835–1840. [CrossRef]
71. Jahelnabi, A.E.; Wu, W.; Boloorani, A.D.; Salem, H.M.; Nazeer, M.; Fadoul, S.M.; Khan, M.S. Assessment the influence of climate and human activities in vegetation degradation using GIS and remote sensing techniques. *Contemp. Probl. Ecol.* **2020**, *13*, 685–693. [CrossRef]
72. Sun, Z.G.; Wu, J.S.; Liu, F.; Shao, T.Y.; Liu, X.B.; Chen, Y.Z.; Long, X.H.; Rengel, Z. Quantitatively assessing the effects of climate change and human activities on ecosystem degradation and restoration in southwest China. *Rangel. J.* **2019**, *41*, 335–344. [CrossRef]
73. Li, H.; Hong, Y.; Deng, G.R.; Wu, R.H.; Zhang, H.Y.; Zhao, J.J.; Guo, X.Y. Impacts of climate change and human activities on net primary productivity of grasslands in Inner Mongolia, China during 1982–2015. *J. Appl. Ecol.* **2021**, *32*, 415–424.

74. Duan, X.; Shi, X.; Li, Y.; Rong, L.; Fen, D. A new method to calculate soil loss tolerance for sustainable soil productivity in farmland. *Agron. Sustain. Dev.* **2017**, *37*, 1–13. [CrossRef]
75. Animal Husbandry Bureau of Yunnan Province. *Yunnan Grassland Resources*; Guizhou People's Press: Guiyang, China, 1989.